



1 **A novel database of Antarctic meteorological extremes over key ice shelves during**
2 **1995-2023**

3 Ian Simpson¹, Edward Hanna¹, Ryan S. Williams², Linh Luu^{1,3,4}, Andrew Orr², Julie M. Jones⁵, Xavier
4 Fettweis⁶, Jose Abraham Torres Alavez⁷, Ole Bøssing Christensen⁷, Ella Gilbert², Sid Gumber², Christoph
5 Kittel⁸, Sihan Li⁵, Damien Maure⁶, Ruth Mottram⁷, Tony Phillips², Willem Jan van de Berg⁹, Kristiina Verro⁷

6 1. *Department of Geography, College of Health and Science, University of Lincoln, UK*

7 2. *British Antarctic Survey, Cambridge, UK*

8 3. *Oxford Sustainable Law Programme, Smith School of Enterprise and the Environment, University of*
9 *Oxford, Oxford, UK*

10 4. *Vietnam Institute of Meteorology, Hydrology and Climate Change, Hanoi, Vietnam.*

11 5. *School of Geography and Planning, University of Sheffield, UK*

12 6. *SPHERE research unit, Department of Geography, University of Liège, Liège, Belgium*

13 7. *Danish Meteorological Institute, Copenhagen, Denmark*

14 8. *VRIJE Universiteit, Brussels, Belgium*

15 9. *Institute for Marine and Atmospheric Research, Utrecht University, Utrecht, Netherlands*

16 Correspondence to: Ian Simpson (ISimpson@lincoln.ac.uk)

17

18
19 **Abstract**

20 The climate of Antarctica is showing increasing signs of being impacted by the warming trend in global
21 temperatures, which has potential to result in accelerated break up of key ice shelves, which would contribute to
22 global sea level rise. Here, we present a novel database of Antarctic extreme weather events over a selection of
23 key ice shelves (Larsen, George VI, Wilkins, Abbot, Thwaites, Totten, Amery, Lazarev), using simulations from
24 four regional climate models (RCMs: RACMO2, HCLIM, MetUM and MAR), driven by the ERA5 reanalysis,
25 examining surface air temperature, precipitation, wind and surface pressure. In addition, we examine trends in
26 the frequency of extreme events above or below specified thresholds (5th, 10th, 50th, 90th and 95th percentiles)
27 and spatial atmospheric circulation and temperature anomaly patterns over Antarctica that are commonly
28 associated with extreme events over key ice shelves. The RCM simulations have been compared with station
29 observations close to the ice shelves, and we developed regressions to estimate simulated values during periods
30 when only one or two of the RCMs were available.

31

32 **Keywords:** Antarctica, climate change, extreme weather events, regional climate models

33



34

1. Introduction

35 There has been a growing amount of research into Antarctic extreme weather events in recent years, particularly
36 given the potential for them to contribute to the break-up of key ice shelves. For example, high temperature events
37 generate surface melting (Orr et al. 2023), which result in surface meltwater ponds over many ice shelves in
38 austral summer. This can result in hydrofracturing (vertical fracturing) if the meltwater penetrates downward and
39 enlarges existing fractures in the ice shelf (Scambos et al. 2000), which can potentially result in the break-up and
40 collapse of the ice shelf (Lai et al. 2020). Strong winds can fuel ocean swells and waves and removal of nearby
41 sea ice, which make the ice shelves susceptible to calving, and are also commonly associated with a warming
42 föhn effect in the lee of high ground (Massom et al. 2018). On the other hand, extreme precipitation events, which
43 predominantly fall as snow, tend to add to the surface mass balance over Antarctica and can offset ice mass losses
44 caused by melting, and to reduce surface meltwater ponding (van Wessem et al. 2023).

45 The ice sheet mass balance over Antarctica has turned negative since the 1990s, with increased ocean-driven
46 melting of ice shelves (Otosaka et al. 2022). Warm ocean currents also exacerbate increased melting and ice sheet
47 collapse (Hanna et al. 2024). While the break-up of ice shelves does not directly cause sea level rise, the Antarctic
48 ice shelves help to reduce the rate of flow of the Antarctic ice sheet into the ocean (buttressing) and to have the
49 effect of shielding the ice sheets and glaciers from warm ocean currents, which limits Antarctica's contributions
50 to global sea level rise (Wang et al. 2025), and so their disintegration contributes indirectly to sea level rise.

51 Atmospheric circulation patterns that commonly contribute to extreme weather events include variations in the
52 Southern Annular Mode (SAM), the climatological Amundsen Sea Low and occurrence of atmospheric river
53 events (Kolbe et al. 2026). The SAM is the leading mode of atmospheric circulation variability in the extratropical
54 Southern Hemisphere (Rogers and van Loon, 1982, Thompson and Wallace, 2000) . A positive SAM sees a
55 poleward shifted jet stream and intensification of the westerlies, which is linked with warming in the Antarctic
56 Peninsula but cooling in central Antarctica (King et al. 2023). The Amundsen Sea Low is a dominant low pressure
57 centre in the Amundsen Sea, where a weaker Amundsen Sea Low can lead to warm water intrusions into the ice
58 shelves, contributing to melt (Hall et al. 2025).

59 Atmospheric rivers are narrow bands of abundant moisture and precipitation, associated with the poleward
60 transport of air masses by hundreds of kilometres. These deliver persistent precipitation near windward coasts
61 and strong föhn effects on the leeward side of high ground, such as over the eastern Antarctic Peninsula and the
62 Larsen C Ice Shelf (Clem et al. 2022), and can result in exceptional warmth and precipitation in affected areas
63 (Siegert et al. 2023). For example, the unusually extensive calving of the Brunt Ice Shelf in February 2021, which
64 resulted in the A74 iceberg breaking off, was associated with a very deep depression which transported warm
65 moist air into the region (Francis et al., 2022).

66 One particularly extreme example was the event in March 2022, which resulted in temperature anomalies (relative
67 to the long-term average) well in excess of 30°C over some regions (Wille et al. 2024a). Anomalous easterly
68 winds, associated with a stationary cyclone to the west of the atmospheric river, probably triggered the collapse
69 of the Conger Ice Shelf, as well as exacerbating anomalously low sea ice extent in the region (Wille et al. 2024b).



70 In February 2022, there was also an exceptional warming event over the Antarctic Peninsula (Gorodetskaya et
71 al. 2023). While such events produced rain and exceptional ice melt near the coasts, precipitation fell
72 predominantly as snow across Antarctica as a whole, and so the Antarctic ice sheets ended up with a record high
73 surface mass balance and a positive net mass balance for the first time in records back to 1993 (Clem et al. 2023).

74 Teleconnections that commonly contribute to Antarctic extreme weather events include the El Niño Southern
75 Oscillation (ENSO), and there are also interdecadal variations associated with the Interdecadal Pacific Oscillation
76 (IPO) and the Atlantic Multidecadal Oscillation (AMO) (Pezza et al. 2012, Li et al. 2021). For example, deep
77 convection in the tropical Pacific tends to result in atmospheric circulation anomalies that transport warm, moist
78 air into the Antarctic, often via atmospheric rivers. Strong concurrent El Niño events, which are associated with
79 anomalously high sea surface temperatures in the Pacific Ocean, can strengthen these moist warm air masses and
80 increase the likelihood of extreme summer melting, as has been studied for example in West Antarctica (Nicholas
81 et al. 2017).

82 Since 2009, major calving events have occurred over the ice shelves not just in the Antarctic Peninsula, but also
83 at the Thwaites and Pine Island ice shelves in West Antarctica, and Nansen, Mertz, Brunt, Amery and Conger ice
84 shelves in East Antarctica (Siegert et al. 2023). Interactions between the atmosphere and oceans, especially during
85 extreme atmospheric conditions, as well as the condition of the ice shelves, likely all contribute to iceberg calving
86 and the disintegration of ice shelves. This was the case with the calving of the Amery ice shelf on 25 September
87 2019, which was triggered by a combination of a long-term increase in rifts in the ice shelf and two explosive
88 cyclones which brought atmospheric rivers and strong winds (Francis et al. 2022), as well as with the
89 disintegration of part of the Conger ice shelf which was related to the March 2022 atmospheric river event.

90 The Antarctic Peninsula warmed considerably during the second half of the 20th century, with a temporary
91 cooling during the 2000s and early 2010s, likely associated with a shift in the SAM to a negative state, which is
92 consistent with natural variability (Turner et al. 2016), and then a resumption of the warming since the mid-
93 2010s. Overall, over the Antarctic Peninsula there has been a linear positive trend in temperature of around
94 +0.26 °C per decade over the period 1978-2020 (Carrasco et al. 2021). This has been associated with increased
95 melt ponding over many of the Antarctic Peninsula ice shelves. Larsen A collapsed in January 1995 and Larsen
96 B collapsed in 2002 (Siegert et al. 2023), and there have been several notable disintegration events affecting parts
97 of the Wilkins Ice Shelf, most notably between 28 February and mid-July 2008 (Scambos et al. 2009). In the
98 summer of 2019/20, an exceptional melt event affected the northern George VI ice shelf in the Antarctic Peninsula
99 (Banwell et al. 2021), and to a lesser extent there was also widespread meltwater ponding on the north-western
100 Larsen C, the eastern Wilkins, and the north-western Bach ice shelves. During this spell, a maximum of 18.3 °C
101 was recorded at Esperanza station, which as of March 2026 remains the highest temperature on record on the
102 Antarctic continent, enhanced by a local föhn effect (González-Herrero et al. 2022). Iceberg A68 broke off from
103 Larsen C in 2017, which was one of the largest icebergs on record and raised concerns about potential decreased
104 stability of what remained of Larsen C. While this happened through a natural calving process, it is possible that
105 it may have been exacerbated by the warming climate (Rignot et al. 2021).

106 Despite a continued rise in global temperatures since 1979, the Antarctic sea ice extent showed a small but



107 significant upward trend between 1979 and 2014, reaching a record maximum value on 20 September 2014
108 (Wang et al. 2019). However, Antarctic sea ice extent then declined dramatically between 2014 and 2016, which
109 may have been linked with some exceptionally deep depressions and changes in wind patterns around Antarctica
110 (Wang et al. 2019), leading to a strongly negative SAM (Chan et al. 2025). One stark example of this sort of
111 feedback affected the Weddell Sea in the austral summer of 2016/17 (Turner et al. 2020), starting with record
112 strength westerly winds in September 2016, pushing multi-year sea ice out of the region, and exceptional storms
113 combined with a record negative phase of the Southern Annual Mode (SAM) in September, which also
114 subsequently resulted in above-average ocean temperatures in the region.

115 The Antarctic sea ice extent remained close to record lows after 2016 and dropped further in 2022 and 2023,
116 setting new record lows. This appears to have substantially modified air-sea interactions in the Southern Ocean
117 and increased wintertime ocean heat loss to the atmosphere, and increased atmospheric storm frequency. There
118 is evidence for this triggering a poleward shift in the jet stream (Zhu and Song, 2022). This may be associated
119 with changes in deep ocean currents, and reduced sea ice may increase circumpolar deep water advection onto
120 the Antarctic ice shelves (Josey et al. 2024).

121 There remain gaps in the understanding of the characteristics of the relationships between temperature,
122 precipitation and wind variability and extremes over Antarctic ice shelves and impacts on melt potential due to
123 sparse and unevenly distributed coverage of meteorological observations, and limitations in the resolution of
124 model parametrisations that cannot capture or resolve small scale processes adequately, such as föhn winds and
125 barrier winds (Orr et al. 2023).

126 In this study we produce and discuss a novel database of Antarctic meteorological extremes between 1995 and
127 2023 over a selection of key ice shelves (Larsen, George VI, Wilkins, Abbot, Thwaites, Totten, Amery and
128 Lazarev), examining surface air temperature, precipitation, surface pressure and surface wind speeds, in
129 identifying extreme events (for example, occurrences of exceptionally high temperatures or precipitation totals)
130 over these ice shelves over the 30-year period.

131 We examine recurring atmospheric circulation characteristics associated with these events, and assess whether
132 these extreme events have become more common and more extreme over the period, to provide a basis for
133 improving the understanding of the key triggers for calving and disintegration of the ice shelves and addressing
134 the gaps in the current understanding of these triggers. This study also aims to identify extreme events that have
135 not been widely covered in the current literature, as well as comparing with well-known extreme events that have
136 been widely discussed such as the March 2022 heatwave/atmospheric river event. Without an extremes database,
137 extreme events can get overlooked if they have minimal impacts at the time, but they could, for example,
138 contribute to impacts on ice shelves later on by undermining their stability.

139

140

141



142

2. Data

143 To generate the database of Antarctic extreme weather events, we primarily used evaluation simulations over
 144 Antarctica from the four regional climate models (RCMs) that were used in the PolarRES dataset (Gilbert et al.
 145 2025): RACMO2, HCLIM, MetUM and MAR. PolarRES was a multi-model ensemble run over the period 2000-
 146 2019 for Antarctica and the Southern Ocean, to help investigate the ocean-atmosphere-ice interactions in the
 147 Antarctic region in understanding how the Antarctic climate system may evolve with global and regional climate
 148 change. Each model used the same domain, resolution, forcing and time period, thus providing a mini-ensemble
 149 of RCMs covering Antarctica and the surrounding area. In some cases, we were able to obtain updated versions
 150 of the models and runs for a longer span of years. The details of these models are given in Table 1.

151 RACMO version 2.4 has been shown to perform well for variables including the surface mass balance,
 152 temperature and wind speed (van Dalum et al. 2025). HCLIM has been shown to represent precipitation better
 153 than the older HIRHAM5 model especially over steep mountains (Belušić et al. 2020), but has a known warm
 154 bias over the ice shelves, though in the PolarRES simulations, none of the four models performed any better or
 155 worse than the others overall (Gilbert et al. 2025).

156 All four models were forced by the ERA5 reanalysis (Hersbach et al. 2020). We did not use ERA5 directly in
 157 this study as ERA5 is at considerably lower horizontal resolution (~30 km) which means that localised
 158 topographic effects are more likely to be missed by the ERA5 reanalysis, and small-scale circulations such as
 159 cloud processes may also be better resolved.

Regional climate model	Version (if named)	Time period	Horizontal resolution
RACMO2	2.4pl	1995-2023	12 km
HCLIM		1995-2020	11 km
MetUM		2000-2020	11 km
MAR	3.13	2000-2020	12 km

160

Table 1. Characteristics of the RCMs used in the study.

161

162 To help validate the regional climate models against observations, we used automatic weather station data,
 163 obtained from BAS, using the READER dataset (Turner et al. 2004). Monthly data were obtained from
 164 <https://www.bas.ac.uk/project/reader/#data> and daily and sub-daily data were obtained via
 165 https://legacy.bas.ac.uk/met/READER/ANTARCTIC_METEOROLOGICAL_DATA/. The stations used,
 166 which were chosen due to their continuous long running records and their position on or adjacent to three of the
 167 key ice shelves, are shown in Figure 1. For this study we did not use the AntAWS dataset (Wang et al. 2022) as
 168 the highest resolution of AntAWS data that we had was 3-hourly, while the READER data are available at up
 169 to hourly resolution. Data from one of the three sites used, Fossil Bluff are only available from 2008 at finer
 170 than daily temporal resolution from AntAWS, while regular daily or sub-daily READER data for Fossil Bluff
 171 start in 2005. As precipitation data are not as reliable at Antarctic stations (for example issues due to blowing
 172 snow) it was not possible to validate the model simulations of precipitation over Antarctica, but validation of



173 surface air temperature, pressure and winds proved possible by comparing station observations against RCM
174 simulations for the corresponding model(nearest neighbour) grid cell.

175 To validate the RCMs, we compared station observations at Fossil Bluff (on the edge of the George VI ice shelf
176 in the Antarctic Peninsula), Larsen Ice Shelf (also Antarctic Peninsula) and Amery G3 (Amery Ice Shelf, East
177 Antarctica) against the model simulations of conditions at the grid box corresponding to those weather station
178 sites, to provide some indication of the models' accuracy. George VI was selected as the first case study for this
179 because of its position within the Antarctic Peninsula, its close proximity to a long-standing station at Fossil
180 Bluff (which has continuous records from 2006, and partial records since 1961), and as a recent record breaking
181 melt event occurred over the ice shelf during the summer of 2019/20 (Banwell et al. 2021). Larsen Ice Shelf has
182 continuous records from 1985 to 2016, providing an overlap of up to 21 years with the RCMs, and Amery G3
183 has continuous records from 1999 to 2011.

184 For wider context, for example when examining extreme temperature and precipitation patterns over Antarctica
185 associated with extreme months that were identified by the RCMs, we used plots derived from the ERA5
186 reanalysis (Hersbach et al. 2020).

187

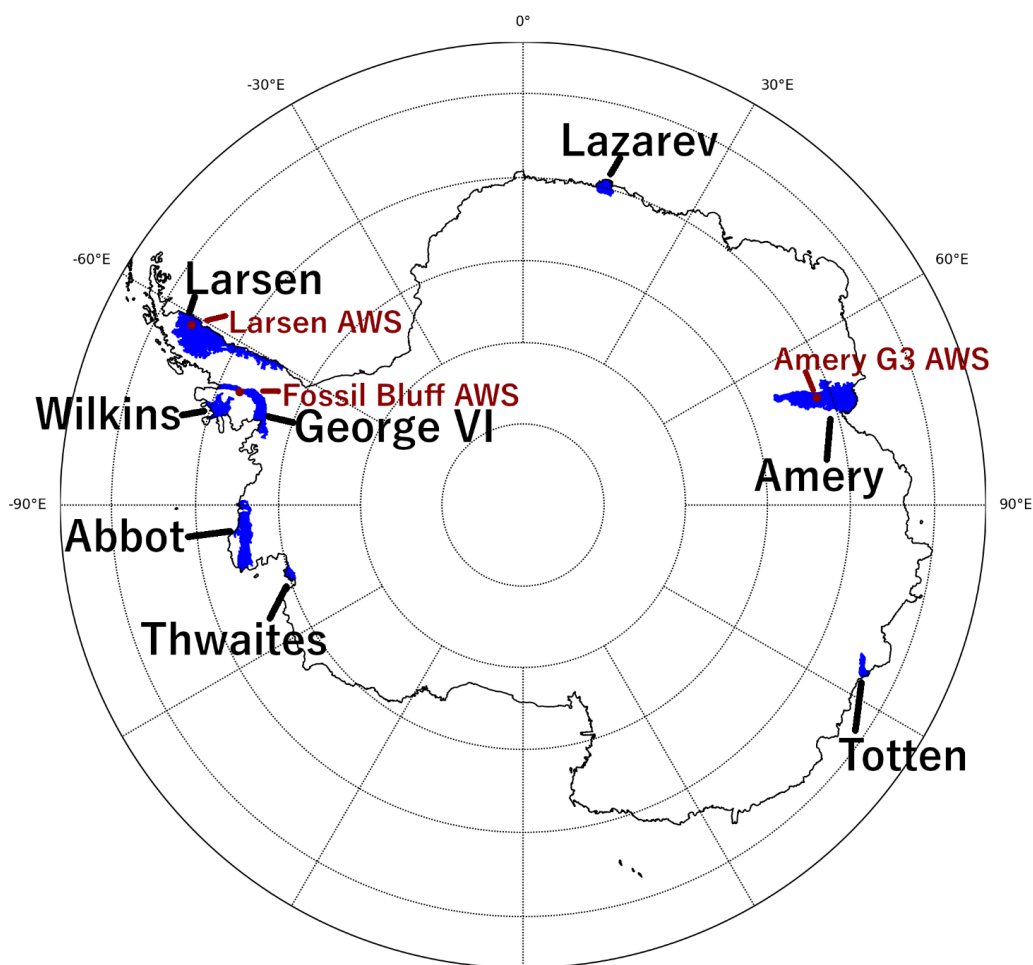
188

189

190

3. Methods

191 High resolution vector polygons of the Antarctic coastline were obtained via Gerrish et al. (2020). From these,
192 we extracted the polygons that corresponded to a selection of key Antarctic ice shelves, which were used as
193 masks for analysis of the areal mean model simulated values of temperature, precipitation, surface pressure and
194 winds. Figure 1 gives an example of the high resolution polygon for the George VI ice shelf.



195

196 Figure 1 The high resolution vector polygons corresponding to the ice shelves considered in the study, plotted
197 on a map of Antarctica. The three automatic weather stations used in the study are also shown.

198

199 Using the vector polygons from Gerrish et al. (2020), we extracted the grid cells that corresponded to a selection
200 of key Antarctic ice shelves (Table 1), and calculated the daily mean temperature, precipitation, surface pressure
201 and surface wind speeds averaged over the ice shelves, from hourly acquired data, for each of the four RCMs. In
202 each case the default rotated pole coordinates were converted to actual latitude and longitude points, temperatures
203 were converted to degrees Celsius, precipitation to mm day^{-1} , surface pressure to hPa and surface wind speeds to
204 m/s , also combining the u and v wind vectors to obtain the overall wind speeds. Hourly values were averaged or
205 summed to daily before calculating climatology and extremes.

206



207 We developed a database of extreme weather events for Antarctic ice shelves, defining extremes as either one
208 day exceeding the 2nd, 5th, 95th or 98th percentiles, or three consecutive days exceeding the 10th or 90th
209 percentiles, for each day of the year. The one day exceeding the higher percentiles was chosen because the
210 standard index which uses three consecutive days above the 90th percentile or below the 10th percentile may
211 miss extreme events which were of shorter duration, but still potentially impactful over ice shelves. This was
212 applied to each of the four variables (surface temperature, precipitation, surface pressure and surface wind speed).

213 Both a multi-model mean and ensemble approach were used. For the multi-model mean approach, for the
214 common period 2001-2019, for which data from all four RCMs were available, daily values of temperature,
215 precipitation, surface pressure and surface wind speed were generated based on the ensemble mean of the four
216 RCMs. Percentiles for each day of the year were calculated based on this period 2001-2019, again based on the
217 mean of the four models. In addition, in cases where not all of the models were available, we developed linear
218 regressions of the form $y = ax + b$, where y is the estimated mean value based on the four models, and x is the
219 value for the combination of models that is available, for each day of the year. This was done to estimate the
220 differences between the estimated mean value using only one, two or three of the RCMs, and the estimated mean
221 value based on the mean of the four RCMs. For periods (1995-2000 and 2020-2023) when some RCMs were not
222 available, we applied the regressions to the mean of the models that were available for those periods, to provide
223 an estimate of daily values that corresponds roughly to the result that may have been obtained from the mean of
224 all four models, to retain consistency with the daily percentiles that were calculated over 2001-2019.

225 For the ensemble based analysis, percentiles for each day of the year were generated individually for each model
226 for the common period 2001 to 2019, and each model's simulated daily value was compared against the
227 percentiles of that model's own distribution, so that extreme events could be assessed on a model by model basis.
228 They also provide counts of the number of models that exceeded particular thresholds for a given day, for we can
229 generally have greater confidence in an extreme event if it was picked out by multiple RCMs, and especially if
230 all four RCMs were available and pinpointed a particular extreme event. We calculated daily mean climatologies
231 and percentiles for each ice shelf over all of the years from 2001-2019. To estimate the mean climatology while
232 removing excess noise from the data, we applied a 3-point harmonic filter, following Bracegirdle et al. (2024),
233 to the mean climatology, including the percentiles and the mean. For all ice shelves, an extreme event is defined
234 relative to the smoothed percentiles (for example. 90th, 95th). We initially attempted analysis based on a 5-day
235 moving average of the percentiles, but determined that, given the relatively short time span of observations, the
236 5-day moving average was not sufficient to remove the noise in the daily data associated with natural short-term
237 variability. For example, this issue arises when daily percentiles are heavily influenced by one or two extreme
238 events in a given year, which serves to obscure the thresholds corresponding to extreme events when performing
239 an analysis of extremes above or below certain percentile thresholds, due to undersampling of the climatology
240 (Risien and Chelton 2008, Narapusetty et al. 2009). It is also important to avoid over-smoothing and filtering
241 out periodic variability that may be down to regional climate characteristics, so we determined that the 3-point
242 harmonic filter was an optimal compromise.

243 We also derived monthly, seasonal and annual time series of temperature, precipitation, surface pressure and



244 surface wind based on the four RCMs, including the individual RCM outputs and the mean of the four models.
245 In addition, we produced time series of counts of extreme events by year and by season. Each of these series were
246 compared with seasonal and annual time series of the El Nino Southern Oscillation (ENSO), Southern Annular
247 Mode (SAM) and sea ice extent in the seas adjacent to the ice shelves (all derived from monthly data) to provide
248 some context regarding the relationships between these modes of variability and mean and extreme weather over
249 the ice shelves. The sea ice extent data were obtained from the National Snow and Ice Data Center (NSIDC),
250 while SAM time series were obtained from the British Antarctic Survey, based on the methods of Marshall et al.
251 (2003). ENSO data, based on the Multivariate ENSO Index Version 2, were obtained from the National Oceanic
252 and Atmospheric Administration (NOAA): see Zhang et al. (2019).

253 When validating the RCMs by comparing with station observations, we extracted the models' estimated height
254 above sea level for the corresponding grid point and applied a correction of 8°C per kilometre (as used for
255 example by Hanna et al. 2011 in assessing Greenland Ice Sheet mass balance) to correct for the discrepancies, as
256 due to model resolution and the variable topography around the edge of the ice shelves, the models commonly
257 overestimate the height above mean sea level.

258 To validate the RCM simulations, for the initial analysis, we compared station observations from automatic
259 weather stations with over 10 years of data within the 1995-2023 period that are located on or adjacent to key ice
260 shelves. We determined the estimated elevation of the grid point from the surface elevation fields from the RCMs
261 for basis of comparison as, particularly in regions of variable topography, the RCMs are prone to smoothing out
262 topography and overestimating elevations. The true elevation of Fossil Bluff is 66m above mean sea level, but
263 RACMO, HCLIM, MetUM and MAR had the corresponding grid point at 227m, 271m, 109m and 150m
264 respectively. For the Larsen Ice Shelf site, there was less bias, with RACMO, HCLIM, MetUM and MAR
265 simulating heights of 37m, 35m, 0m and 33m, compared with the actual site elevation of 43m. For the Amery
266 G3 site, again MetUM had the simulated height at 0m but the other three models had the height simulated within
267 5m of the observed height of the site (84m).

268 In addition, we also examined the relationships between mean temperature, precipitation, pressure and wind, and
269 counts of extreme events, with the sea ice extent over the seas adjacent to the ice shelves, together with the SAM
270 and ENSO indices. For the sea ice analysis, rather than taking the overall Antarctic sea ice extent, which would
271 mask regional variations in the sea ice extent, we created annual and seasonal series of Antarctic sea ice extent
272 for the Amundsen-Bellinghshausen, Indian, Pacific, Ross and Weddell Seas from the National Snow and Ice Data
273 Center (NSIDC), based on Meier et al. (2023), so that seasonal and annual data for each ice shelf could be
274 compared with the overall sea ice extent for the nearest adjacent sea.

275

276

277

278



279

4. Results

280

4.1 RCM comparisons with station observations

281

Variable	RACMO	HCLIM	MetUM	MAR
Fossil Bluff				
Correlations				
Temperature (°C)	0.89	0.94	0.94	0.89
Pressure (hPa)	0.99	0.99	0.99	0.90
Wind (m/s)	0.71	0.70	0.80	0.27
RMSE				
Temperature (°C)	3.86	3.23	7.38	4.96
Pressure (hPa)	33.1	29.2	13.4	18.6
Wind (m/s)	2.00	2.17	1.93	3.03
Larsen Ice Shelf				
Correlations				
Temperature (°C)	0.94	0.95	0.96	0.91
Pressure (hPa)	0.90	0.89	0.99	0.82
Wind (m/s)	0.61	0.65	0.75	0.50
RMSE				
Temperature (°C)	3.70	3.51	3.01	4.44
Pressure (hPa)	5.20	6.61	1.55	6.44
Wind (m/s)	2.42	1.92	1.80	2.37
Amery G3				
Correlations				
Temperature (°C)	0.96	0.95	0.97	0.96
Pressure (hPa)	0.98	0.97	0.99	0.89
Wind (m/s)	0.84	0.79	0.88	0.72
RMSE				
Temperature (°C)	3.20	6.36	2.37	2.93
Pressure (hPa)	8.84	11.2	1.72	11.1
Wind (m/s)	4.32	6.05	5.08	4.63

282

Table 2. Correlations between the model simulations of daily values and Antarctic automatic weather station observations used for comparison with RCMs at the three sites, over 2005-2023 (Fossil Bluff), 1995-2016 (Larsen Ice Shelf) and 1999-2011 (Amery G3). The root mean square error of the correlations (RMSE) is also shown. Due to the large sample size (daily data), all correlations were significant at the 99% level ($p < 0.01$).

286

287



288 Correlations with temperature observations at each of the sites were reliably high ($p < 0.01$ in all cases), but
289 higher in the case of HCLIM and MetUM than for/of MAR. For surface pressure, correlations with observations
290 were higher, but lower for MAR than for the other models. For surface wind speed, correlations with observed
291 values were lower, but again substantially lower in the case of MAR than the other models, particularly in the
292 case of Fossil Bluff. The lower correlations with wind speed observations can be explained by the relatively
293 limited model resolution failing to capture variations in topography that create localised differences in wind
294 speeds depending on the wind direction and the specific pressure pattern. The root mean square error (RMSE)
295 varied between models depending on the ice shelf, but the larger RMSE for HCLIM compared with the other
296 models in the case of Amery G3 may be linked with the summer warm bias shown in Figure 2 (see also Fig. 9 in
297 Gilbert et al., 2025).

298 A further comparison (see Figure 2) to test the model simulations of extreme weather events, was to plot daily
299 station temperature, and the 95th percentile of the station temperature (x axis), and model simulations of daily
300 temperature minus daily station temperature. For temperature (Figure 2), the results comparing Amery G3 with
301 observations particularly show HCLIM having a strong warm bias, but mainly on occasions when temperatures
302 at Amery G3 were between 0 and 10°C below the 95th percentile, and not when temperatures exceeded the 95th
303 percentile. Further analysis which broke the results down by season (Figure 3) suggest that the HCLIM warm
304 bias comes mainly from summer (DJF). The plots for the other three models in Figure 2 suggest a small tendency
305 to underestimate extreme high temperatures, except in the case of Fossil Bluff, where MetUM has a large
306 underestimate especially for low temperatures, and MAR a large overestimate.

307 The HCLIM warm bias proved to be less strong when comparing the model simulations with the observations
308 over Fossil Bluff at the edge of the George VI ice shelf, and over the Larsen Ice Shelf, but there was still a warm
309 bias in summer, with values mostly in the range of 2 to 10 °C, rather than approaching 20 °C as in the case of
310 Amery. This implies that HCLIM should be used with caution when assessing the magnitude and likely impacts
311 of warm summer events over Antarctica.

312

313

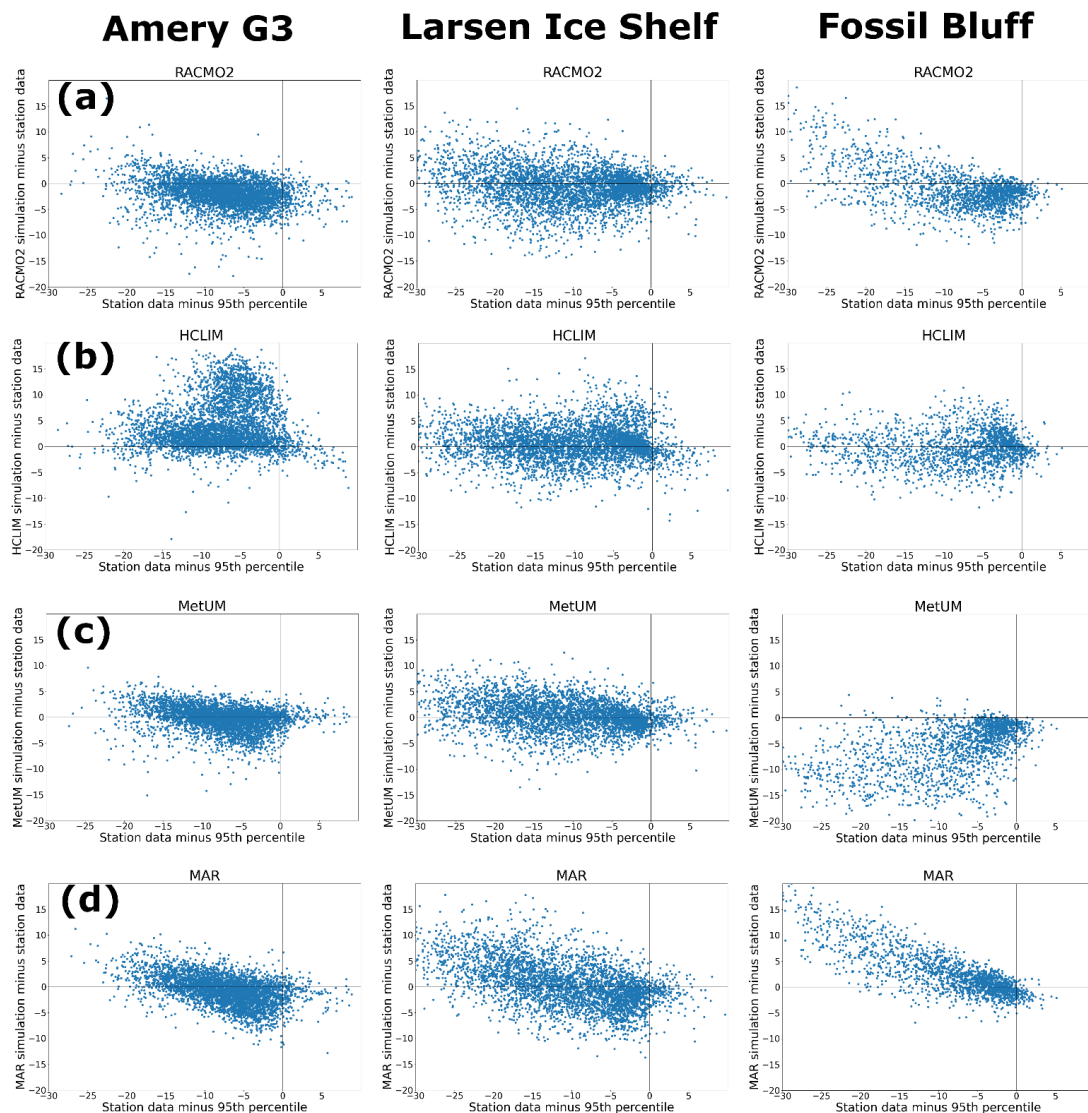


Figure 2. Comparisons between the station temperature minus the 95th percentile of the station temperature (x axis), and model simulations of daily temperature minus daily station temperature (y axis), for (a) RACMO2, (b) HCLIM, (c) MetUM and (d) MAR, for all data. Amery G3 data were available over 1999-2011, Larsen Ice Shelf over 1985-2016, and Fossil Bluff over 2005-2023. Points to the right of the vertical line indicate daily temperatures that exceeded the 95th percentile of the model data. Temperatures are in °C.

314

315

316

317

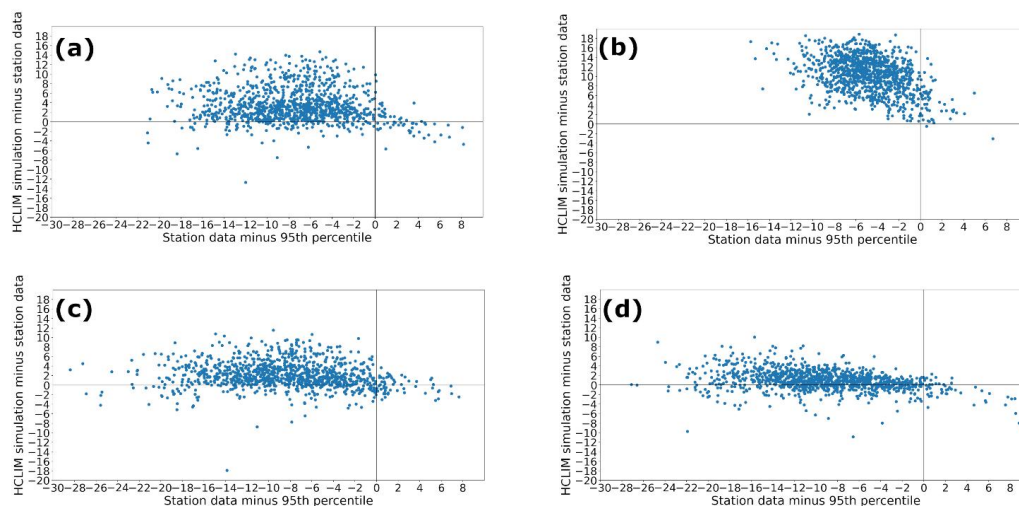


Figure 3. Comparisons between daily station temperature and the 95th percentile of the station temperature (x axis), and HCLIM simulations of daily temperature minus daily station temperature (y axis), for Amery G3, for (a) spring, (b) summer, (c) autumn and (d) winter. The warm bias is most evident in summer and reduces to near zero in winter. Temperatures are in °C.

318

319 The results for surface pressure (not shown) show greater consistency between the models for Fossil Bluff, but
320 with some evidence of HCLIM and MetUM overestimating the extremes of pressure. For wind speed (not shown),
321 the graph for MAR suggests that MAR underestimates extreme high wind speeds at Fossil Bluff. For the Larsen
322 and Amery sites, the results consistently pointed to the models being consistent with observations or slightly
323 underestimating the extremes.

324

325 4.2 The extremes database

326

327 4.2.1 Consistent model differences across the different ice shelves

328 When considering the percentile distribution of the individual RCMs, one feature that stands out is that HCLIM
329 consistently simulates higher temperatures than the other three models during the summer months, especially
330 January, and the difference is largest for the cold extremes. For example, averaged over the Abbott ice shelf over
331 the month of January (Tables 3 and 4), the 2nd percentile averages -10.1°C according to RACMO2, -10.0°C
332 according to MetUM, -8.3°C according to MAR, but the HCLIM value is -3.0°C. HCLIM also simulates higher
333 high extreme temperatures, but to a lesser extent, with HCLIM tending to produce 90th, 95th and 98th percentiles
334 that are 1 to 2°C higher than the other models, as opposed to as much as 7°C higher for the 2nd percentile. The
335 difference is present for all ice shelves, but is stronger over some ice shelves than over others. For example, over



336 the Antarctic Peninsula ice shelves at Larsen and George VI, HCLIM simulates warm extremes that are around
 337 3°C higher than the other models, and over Amery the 98th percentile of HCLIM is over 8°C higher than for the
 338 other models. This does not appear to bias the statistical distribution of extreme events, as events that appear as
 339 extremes on the other three models also predominantly appear in the HCLIM extremes. However, it implies that
 340 HCLIM has some temperature biases that may affect simulations of surface melt over some of the ice shelves,
 341 due to simulating longer periods with above freezing temperatures and potentially rain instead of snow. Similar
 342 HCLIM temperature biases were also found over various regions of Antarctica in the PolarRES model analysis
 343 of Gilbert et al. (2025). Other consistent issues include a tendency for MetUM and RACMO2 to simulate a larger
 344 range of temperatures (for example, higher 95th percentile, lower 5th percentile) than the other models, with
 345 MAR simulating the lowest range, which is consistent with the results of the extremes analysis in section 4.1.

346

Model	Larsen	George VI	Wilkins	Abbot	Thwaites	Totten	Amery	Lazarev
RACMO2	-6.6	-7.6	-6.1	-10.1	-10.7	-10.7	-10.8	-10.0
HCLIM	-2.7	-1.6	-3.0	-3.1	-3.7	-3.5	0.5	-2.9
MetUM	-7.5	-8.8	-8.0	-10.1	-10.4	-8.6	-3.9	-10.2
MAR	-7.6	-6.5	-7.5	-8.4	-8.7	-11.0	-12.4	-12.2

Table 3. Model simulated mean daily 2nd percentile temperatures in degrees Celsius for the month of January, over each of the ice shelves.

347

Model	Larsen	George VI	Wilkins	Abbot	Thwaites	Totten	Amery	Lazarev
RACMO2	1.0	1.3	1.8	0.5	-0.4	-0.2	-1.0	-0.8
HCLIM	4.5	2.7	2.0	1.4	1.5	0.4	8.7	2.4
MetUM	0.4	1.3	1.3	0.5	0.4	-0.1	0.4	-0.4
MAR	1.6	1.7	1.3	-0.5	-0.8	-0.0	-2.0	-1.6

Table 4. As Table 3 but showing the mean daily 98th percentile temperatures for January

348

349 A sample plot of the four models' simulations of temperature over the Larsen ice shelf during the calendar year
 350 2006, which includes the percentile distributions, is shown in Figure 4. All four models pick out an extreme
 351 winter warm spike at the end of June 2006, and simulate temperatures exceeding the 95th percentile in several
 352 spells during January and February 2006. The HCLIM summer warm bias is also evident over Larsen, with 95th
 353 and 98th percentiles coming out close to 5°C while the other three models produce 95th and 98th percentiles
 354 close to 0°C.

355

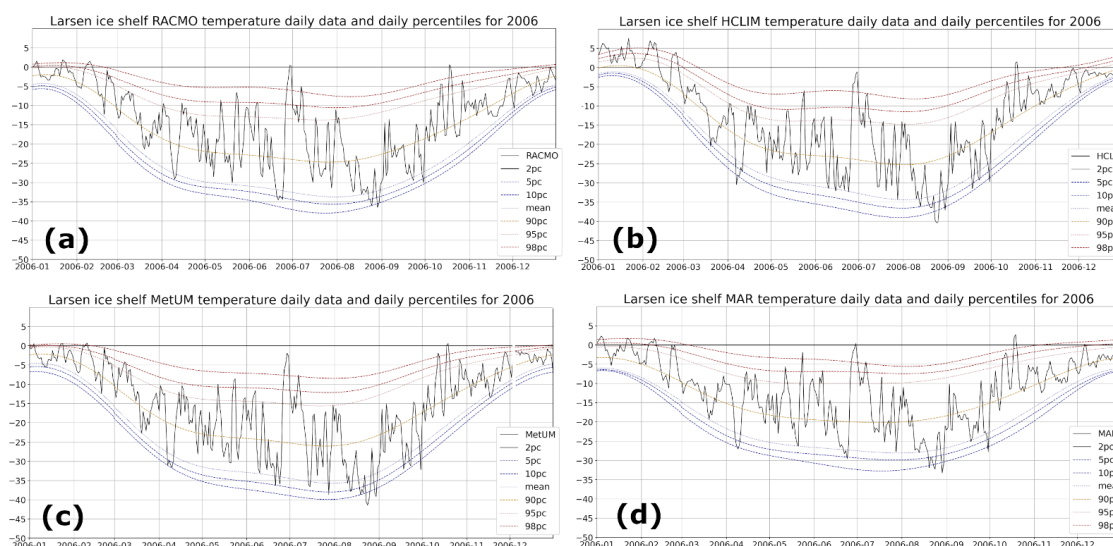


Figure 4. Model simulations of daily surface temperature (°C) over the Larsen ice shelf for 2006, using (a) RACMO2, (b) HCLIM, (c) MetUM and (d) MAR, and daily percentiles for the common period 2001-2019.

356

357 Considering the other three variables (not shown), considering the whole 1995-2023 period in the study, there
358 are no strong systemic differences in extreme values between the models for precipitation, but MAR consistently
359 simulates lower wind speeds than the other models, with RACMO2 simulating the highest wind speeds. For
360 surface pressure, MetUM consistently simulates higher pressure than the other models, typically by around 5
361 hPa, but as with the HCLIM winter warm bias, this appears to be a largely systemic difference that does not affect
362 the detection of extreme events.

363

364 4.2.2 Trends in annual and seasonal mean values and in counts of extreme events

365 Examining trends in annual and seasonal mean values and extremes over the Antarctic ice shelves is currently
366 problematic due to the relatively short time span of the extremes database (1995-2023, 29 years). With a few
367 exceptions, trends in both mean and extreme temperature and precipitation have been weak over the ice shelves
368 over the period. Exceptions include a positive trend in high temperature extremes in spring over Amery, an overall
369 annual (but not seasonal) increase in extreme high precipitation events over Larsen, an increase in extreme
370 summer precipitation events over Thwaites, and a decrease in extreme summer high temperatures over Wilkins.
371 Figure 5 shows the annual and seasonal counts of daily extreme temperatures above the 95th percentile, while
372 Figure 6 is as Figure 5 but for precipitation extremes, both using the model mean. The annual counts of extreme
373 events show signs of an increase in extreme events after 2015, when the overall Antarctic sea ice extent dropped
374 from setting record highs to increasingly setting record lows, but due to regionally large interannual variability
375 2016-2023 is too short a time period to be able to draw clear conclusions from, and not long enough to produce
376 strong overall upward trends in extremes over the period considered. Instead, of more interest are periods of



377 multi-year persistence and variability. Most of the ice shelves saw at least one year with an unusually high number
378 of extreme high temperature events during the period 1995-1998, comparable to those of more recent years such
379 as 2016, 2019 and/or 2020, which contributed to the recent extreme years generally failing to result in an overall
380 increasing trend in temperature extremes during the period. The lack of a significant warming trend in the study
381 over the Antarctic Peninsula ice shelves is likely due to the choice of period, which sees relatively warm
382 temperatures early and late and a cooler period around the early 2010s (Turner et al. 2016), and also the high
383 inter-annual temperature variability that characterises the region.

384 Over the Antarctic Peninsula ice shelves of George VI, Larsen, and nearby Wilkins, 1998 and 2016 were extreme
385 warm years, both in terms of mean temperature and extreme high temperature events, but most of the extreme
386 warm events of those years happened in the winter half-year, leading to relatively limited impacts on the ice
387 shelves. Larsen also had a high number of extreme precipitation events in 2017.

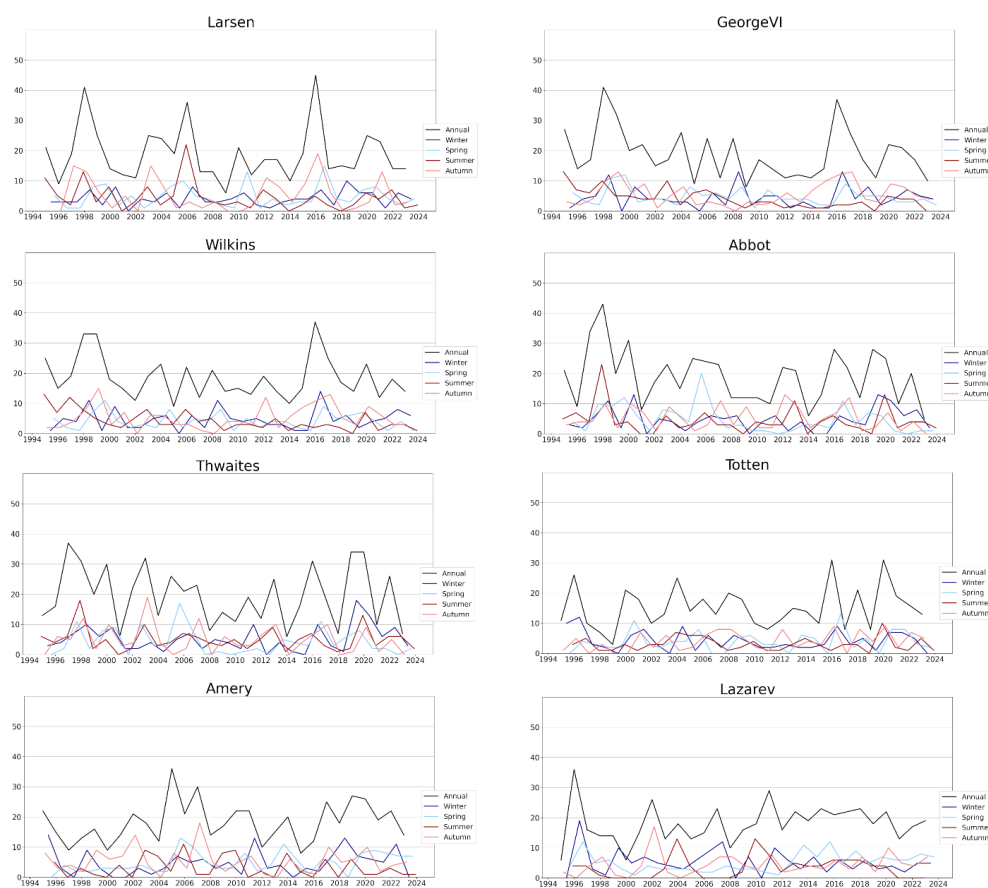


Figure 5. Seasonal and annual counts of daily temperature ($^{\circ}\text{C}$) events (number of days) above the 95th percentile over the eight ice shelves.



389

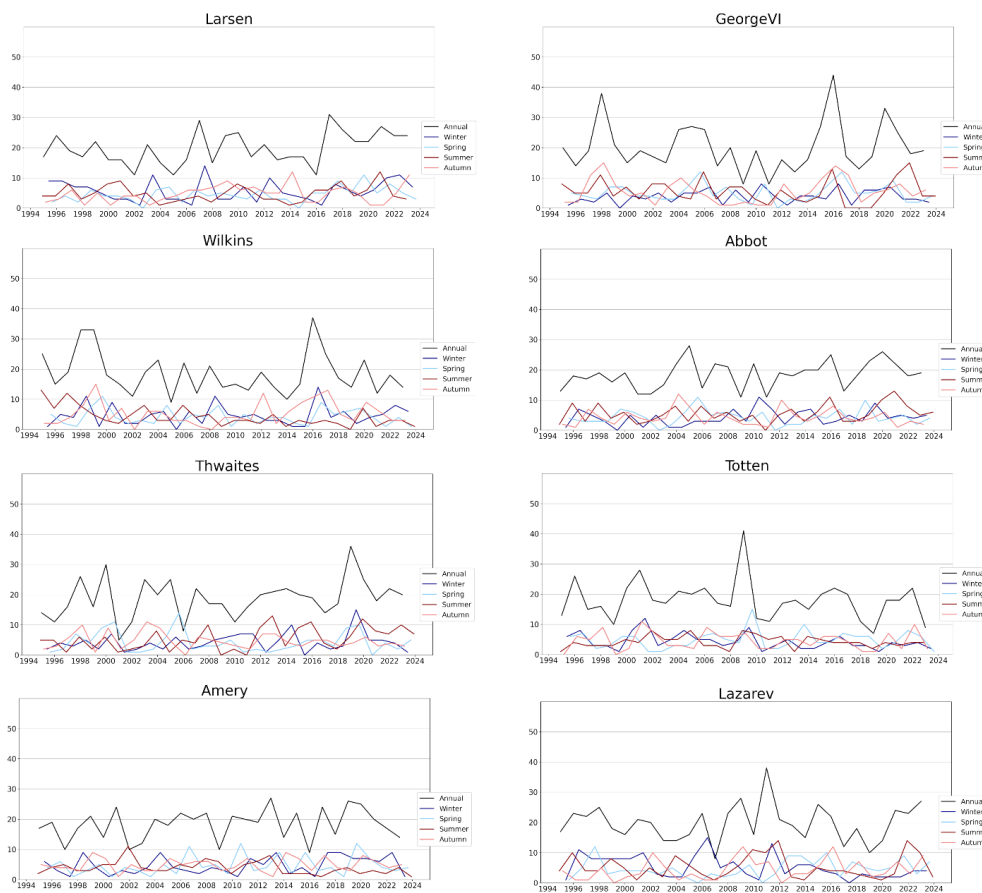


Figure 6. Seasonal and annual counts of daily precipitation (mm) events (number of days) above the 95th percentile over the eight ice shelves.

390

391

392

393

394

395

396

397

398

399



400 Over Thwaites, 2019 stands out as an extreme year, having had the highest number of days with extreme high
401 precipitation, the highest annual mean temperature, and it also had among the highest counts of extreme warm
402 temperature events, but not as high as 1997. Most of the extremes of 2019 were clustered in winter and early
403 spring, but the summer of 2019/20 contained numerous extreme high temperature events. Over Abbot, 2016,
404 2019 and 2020 all had a high number of extreme high temperature events. Breaking it down by season, 2019/20
405 was a recent extreme summer over Thwaites and Abbot, but again not more extreme than several earlier years in
406 the late 1990s and early 2000s.

407 Over Totten, 2016, 2018 and 2020 stand out as having a high number of extreme temperature events, but not as
408 extreme years for precipitation, while recent years do not stand out as having high counts of extreme events over
409 Amery and Lazarev.

410 Comparing the SAM, ENSO and Antarctic sea ice with mean temperature, precipitation, pressure and wind, the
411 results suggest that the SAM is positively linked with both annual mean temperatures and extremes around the
412 Antarctic Peninsula (Table 5), but significantly negatively correlated with annual mean temperature (but in most
413 cases not temperature extremes) over the Totten, Amery and Lazarev ice shelves, bordering the Pacific and Indian
414 Oceans, as was also found by Orr et al. (2023). In spite of the El Nino years of 1998 and 2016 having been
415 exceptionally warm around the Antarctic Peninsula, mean annual temperatures over George VI and Wilkins have
416 significant negative correlations with ENSO. Correlations of annual mean temperature and annual counts of
417 extremes were mostly negatively correlated with sea ice extent, but in most cases not significantly so ($p > 0.05$),
418 and when considering individual seasons (not shown), the relationships were weaker than when examining annual
419 data. Both annual mean precipitation and extreme precipitation events over the 95th percentile were strongly
420 negatively correlated with sea ice extent over Larsen ($p = 0.011$ in both cases), but not the other ice shelves.

421 Over Thwaites, ENSO and sea ice extent proved to be negatively related to extreme high winds over the 95th
422 percentile (Table 8), and there was also a strong negative correlation between sea ice extent and wind extremes
423 over the Totten ice shelf, but otherwise correlations between these indices and extreme winds tended to be weak.
424 The SAM was negatively linked with high surface pressure extremes over the Antarctic Peninsula ice shelves
425 during the period (Table 7). Tables 5 and 6 provide a summary of the correlations between temperature and
426 precipitation and the three potential drivers of extreme weather events.

427

428

429

430

431

432

433

434



Variable	Larsen	George VI	Wilkins	Abbot	Thwaites	Totten	Amery	Lazarev
Mean annual temperature								
ENSO	0.10	-0.38	-0.38	-0.14	0.13	0.10	0.14	0.22
SAM	0.32	0.37	0.44	0.07	0.08	<u>-0.53</u>	<u>-0.50</u>	<u>-0.53</u>
Sea ice extent	-0.20	-0.25	-0.34	<u>-0.63</u>	-0.15	-0.21	0.21	-0.46
Annual count of daily temperature events above the 95th percentile								
ENSO	0.26	-0.13	0.11	0.39	0.38	-0.03	-0.17	-0.03
SAM	0.41	<u>0.48</u>	0.33	-0.07	0.09	-0.11	-0.27	-0.35
Sea ice extent	0.01	-0.30	-0.21	-0.34	-0.37	0.17	-0.08	-0.34

Table 5. Correlations between mean annual temperature and annual counts of daily temperature over the 95th percentile and three potential drivers of extreme events, with bold indicating significance at $p \leq 0.05$, and underline indicating significance at $p \leq 0.01$. Correlations are based on calculating annual mean values of ENSO, SAM and sea ice extent against annual counts of extreme events in the database.

435

Variable	Larsen	George VI	Wilkins	Abbot	Thwaites	Totten	Amery	Lazarev
Mean annual precipitation								
ENSO	-0.46	0.24	0.16	0.00	0.12	-0.16	-0.08	0.02
SAM	0.13	0.41	<u>0.48</u>	0.32	0.04	-0.01	-0.03	0.18
Sea ice extent	<u>-0.47</u>	-0.19	-0.18	-0.32	-0.18	-0.31	0.37	-0.29
Annual count of daily precipitation events above the 95th percentile								
ENSO	-0.16	0.26	0.11	0.02	0.14	-0.16	-0.22	-0.11
SAM	0.00	0.26	<u>0.51</u>	0.25	0.16	0.06	0.06	0.15
Sea ice extent	<u>-0.47</u>	-0.20	-0.29	-0.08	0.02	-0.22	0.04	-0.16

Table 6. As Table 5, but examining mean and extreme precipitation.

436

437

Variable	Larsen	George VI	Wilkins	Abbot	Thwaites	Totten	Amery	Lazarev
Mean annual pressure								
ENSO	0.15	0.28	0.33	0.37	0.34	-0.21	0.05	0.01
SAM	<u>-0.73</u>	<u>-0.72</u>	<u>-0.70</u>	<u>-0.76</u>	<u>-0.76</u>	-0.37	<u>-0.85</u>	<u>-0.82</u>
Sea ice extent	0.24	-0.16	-0.17	-0.06	-0.02	0.02	-0.21	0.07
Annual count of daily pressure events above the 95th percentile								
ENSO	0.21	0.30	0.30	0.04	0.16	-0.30	0.04	-0.35
SAM	<u>-0.60</u>	<u>-0.50</u>	<u>-0.52</u>	<u>-0.59</u>	<u>-0.59</u>	<u>-0.60</u>	<u>-0.63</u>	<u>-0.59</u>
Sea ice extent	0.09	-0.01	-0.07	-0.15	-0.12	-0.16	0.08	-0.03

Table 7. As Table 5, but examining mean and extreme pressure.

438



439

Variable	Larsen	George VI	Wilkins	Abbot	Thwaites	Totten	Amery	Lazarev
Mean annual wind speed								
ENSO	-0.13	-0.33	-0.29	-0.31	-0.34	-0.20	-0.17	-0.23
SAM	0.38	0.44	<u>0.52</u>	0.41	0.39	0.35	0.32	0.33
Sea ice extent	-0.45	-0.01	-0.06	-0.04	-0.01	-0.14	-0.34	-0.46
Annual count of daily wind speed events above the 95th percentile								
ENSO	0.33	-0.17	-0.11	-0.24	-0.38	-0.01	0.03	-0.07
SAM	-0.14	0.09	0.34	0.19	0.24	-0.05	0.03	0.27
Sea ice extent	0.20	-0.26	-0.08	-0.34	-0.36	<u>-0.53</u>	0.06	-0.01

Table 8. As Table 5, but examining mean and extreme wind speeds.

440

441

4.3 Case studies

442

443

4.3.1 Extreme events in the late 1990s and 2000s

444

445 The Larsen A ice shelf disintegrated between January and March 1995, losing half of its floating area in the last
 446 week of January (Royston and Gudmundsson, 2016). This analysis starts only in January 1995, but January 1995
 447 was an anomalously warm month over the Antarctic Peninsula (Figure 7), with two separate warm events where
 448 temperatures over the ice shelf were simulated to be well above freezing and well above the 98th percentile on
 449 two separate occasions during the month – the 9th/10th January and between the 24th and 26th January (Figure
 450 8). There were also exceptionally strong winds, well above the 98th percentile, on the 25th January, indicating
 451 that a substantial storm affected the region. In contrast, most of the rest of Antarctica had temperatures below the
 452 1981-2010 average.

453 Larsen B disintegrated during February and March 2002 (Scambos et al. 2004). Unlike the Larsen A
 454 disintegration, this extremes database suggests that any contribution from surface weather conditions to the
 455 disintegration of Larsen B was probably cumulative rather than caused by individual extreme events (Fahnestock
 456 et al. 2002). Temperatures were persistently above the 1981-2020 long-term average over the Larsen ice shelf,
 457 and the Antarctic Peninsula generally, between mid-September 2001 and early March 2002, but not exceptionally
 458 so. An extreme wind and precipitation event is picked out for 10/11 March 2002, but this was after the period of
 459 peak decline over Larsen B.

460 February 2006 stands out as an extreme month over West Antarctica, a month which saw exceptional melting
 461 over the nearby Peter 1st Island in the Bellingshausen Sea (Thomas et al. 2024). The warmth affected a large
 462 area. The extremes database picks out extreme warm events in February 2006 affecting the Larsen, George VI,
 463 Wilkins, Abbot and Thwaites ice shelves, with two marked ones early and late in the month, also accompanied



464 by unusually high precipitation. Mean sea level pressure anomaly charts from February 2006 (Figure 7) show a
465 strong high pressure anomaly over the Peninsula, shifted south from its position in January 1995. However, this
466 extreme month appears not to have been associated with substantial impacts on the ice shelves of mainland
467 Antarctica., as we are unable to find any relevant reports in the literature. The extremes database also picks out
468 an exceptional winter storm in late June 2006, with exceptionally high temperatures accompanied by high
469 precipitation and strong winds, especially affecting the Peninsula. June 2006 also had a similar mean sea level
470 pressure anomaly pattern to January 1995, with anomalously high pressure off the coast of the Peninsula.
471 However, with temperatures modelled to be just below freezing over Larsen, George VI and Wilkins, it may not
472 have been warm enough to cause substantial melting.

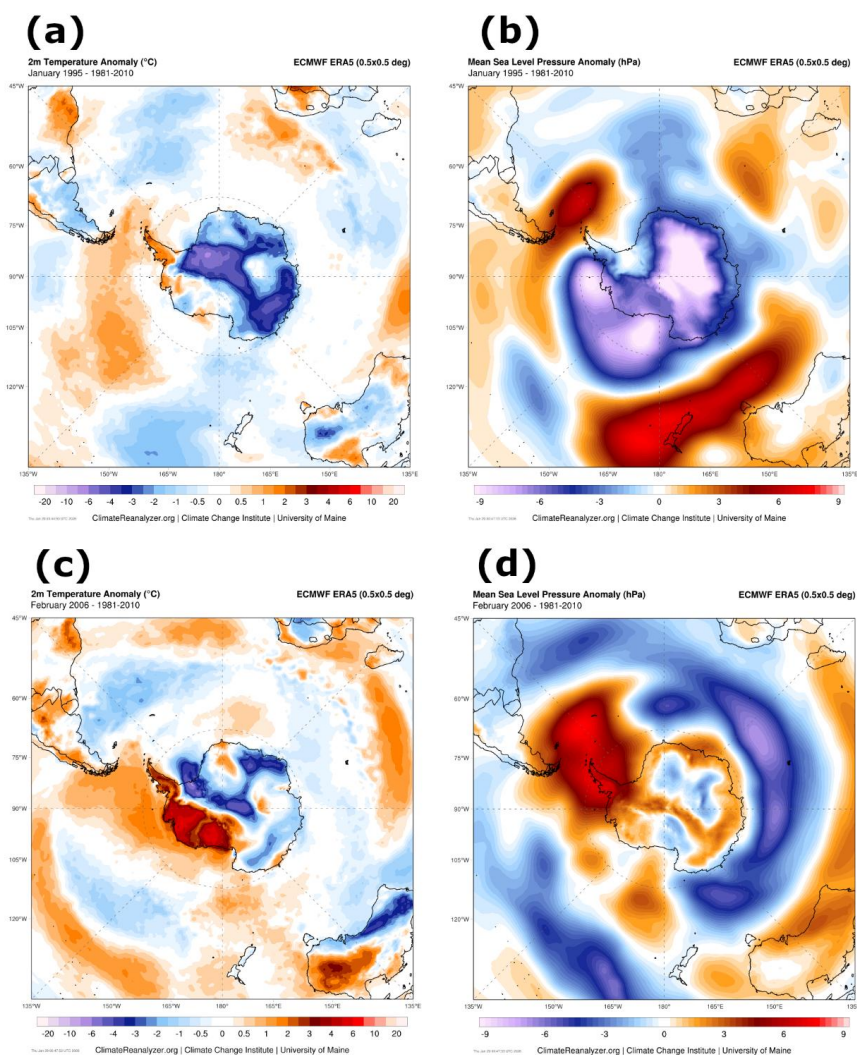


Figure 7. (a) and (b) show the mean 2m temperature anomaly in °C and mean sea level pressure (hPa) anomaly respectively, relative to 1981-2010, for January 1995. (c) and (d) are as (a) and (b), but for February 2006. All charts are courtesy of Climate Reanalyzer.



493 The succession of calving events at the Wilkins ice shelf between February and July 2008 does not appear to
494 have been associated with a particularly extreme year. However, the summer of 2007/08 was generally warmer
495 than average except for a cool first half of January, and there were two temperature spikes in quick succession
496 exceeding the 95th percentile on 11 and 15 February 2008, which could have helped precondition the ice shelf
497 for some melting later in the season.

498

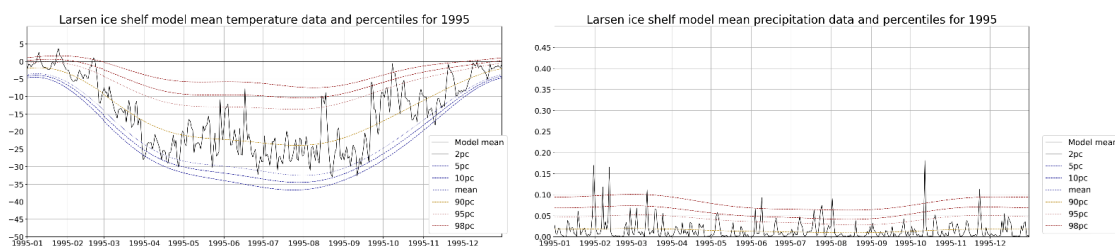


Figure 8. Model simulations of daily surface temperature and daily surface wind speed over the Larsen ice shelf, compared with daily percentiles over 2001-2019, for 1995, based on the mean of the available models (RACMO2 and HCLIM for 1995).

499

500

501

502

4.3.1 Extreme events since 2016

503

504 Although the unusual conditions over the Weddell Sea in the 2016/17 season are not associated with any notable
505 extremes in this Antarctic extremes database, Figure 9a shows that March 2017 showed strong positive monthly
506 temperature anomalies of up to 8°C over West Antarctica and the Peninsula. Again, it was characterised by
507 anomalously high pressure over the coastal Peninsula (Figure 9b), perhaps leading to westerly winds and a föhn
508 effect in some regions. Temperatures were persistently high, and sometimes in excess of the 98th percentile, over
509 Larsen, George VI, Wilkins, Abbot and Thwaites, and averaged over Wilkins the temperature is simulated to be
510 just above freezing on several days during the month. This may have been linked with an exceptionally low
511 Antarctic sea ice extent at the beginning of March 2017, which was particularly low around West Antarctica
512 (Figure 9c, Turner and Comiso, 2017).

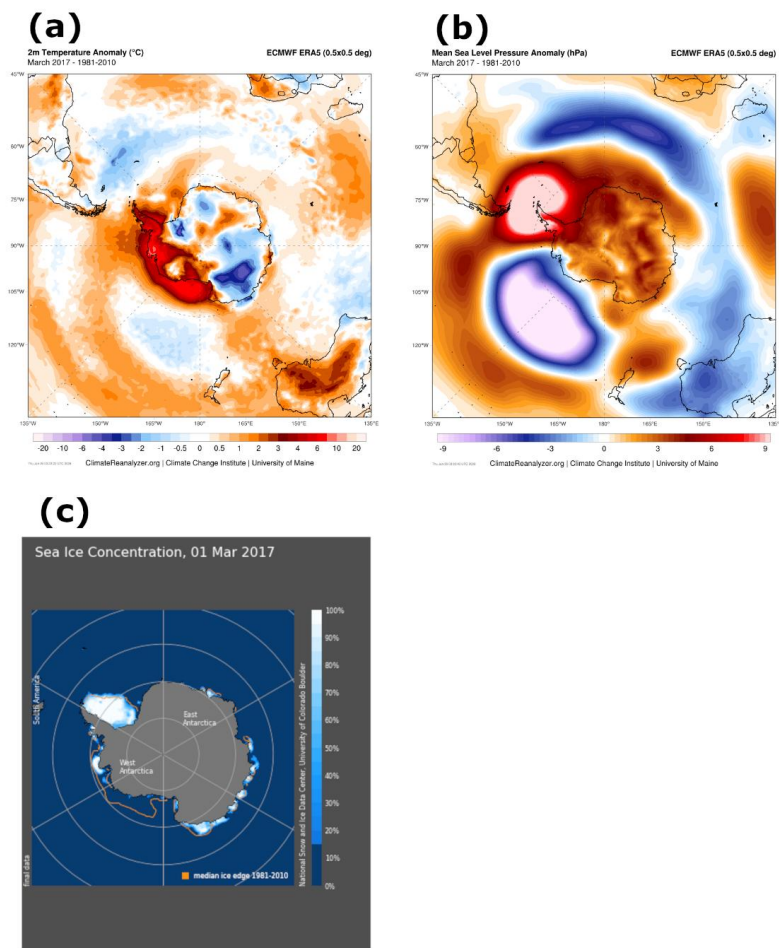


Figure 9. (a) The mean temperature anomaly in °C over Antarctica relative to 1981-2010 for March 2017, courtesy of Climate Reanalyzer. (b) The mean sea level pressure anomaly in hPa over Antarctica relative to 1981-2010 for March 2017, also courtesy of Climate Reanalyzer. (c) Sea ice extent and anomaly on 1 March 2017, courtesy of the National Snow and Ice Data Center.

531

532 The calving event on the Amery ice shelf on 25 September 2019 is not picked out by the extremes database as
533 being associated with extreme temperatures, precipitation or wind, although temperatures were persistently above
534 the 1981-2010 average over Amery during the second half of September 2019, exceeding the 95th percentile on
535 20 September.



536 The summer of 2019/20, which had an exceptional melt over the northern George VI ice shelf (Banwell et al.
 537 2020, Xu et al. 2021), stands out as an extreme summer over the Antarctic Peninsula (Figure 10). Over George
 538 VI, the mean temperature over the ice shelf is simulated to repeatedly reach close to or just above freezing
 539 between late November 2019 and mid-March 2020. An extreme event is picked out over Larsen between 6 and
 540 10 February 2020, with temperatures exceeding the 98th percentile on the 6th, 8th, 9th and 10th, accompanied
 541 by precipitation totals exceeding the 95th percentile (not shown). Over Abbot and Thwaites, the 2019/20 season
 542 also sticks out as an extreme one except for January 2020, which had close to average temperatures.

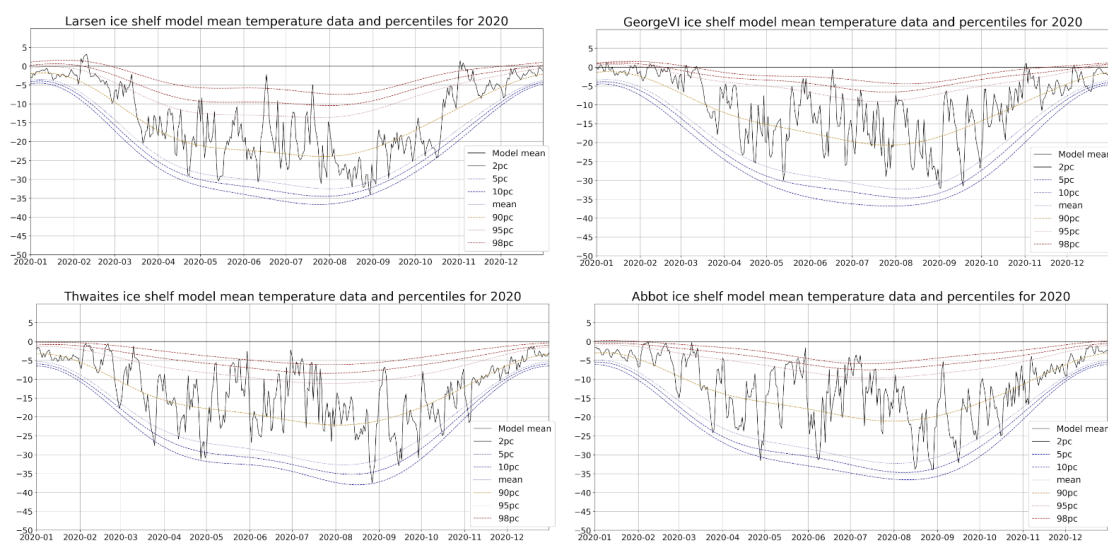


Figure 10. Based on the mean of the available models, simulated daily temperature in °C over the Larsen, George IV, Thwaites and Abbot ice shelves for 2020, and daily percentiles for 2001-2019.

543 As noted in the introduction, there was an exceptional atmospheric river event in March 2022 over East
 544 Antarctica. A caveat when analysing this event is that of the four models used in this analysis, only RACMO2
 545 was available for March 2022. Nonetheless, RACMO2 picked out four consecutive days of temperatures
 546 exceeding the 98th percentile over the Totten ice shelf from 16-19 March 2022 (Figure 11), combined with
 547 unusually strong winds and unusually high precipitation amounts, exceeding three times the 98th percentile.
 548 Temperatures are, however, simulated to be just above -5°C, which is consistent with the observation of Clem et
 549 al. (2023) that rain and extensive melting along the coast was outweighed by snow accumulations inland, leading
 550 to a net increase in the ice mass balance. However, the event produced temperatures that are rarely exceeded in
 551 heatwaves even in high summer, and were a similar atmospheric river event to happen in high summer instead
 552 of March, the impacts may be very different. In addition, the event contributed to the collapse of the nearby
 553 Conger ice shelf (Wille et al. 2024a). Temperature extremes exceeding the 98th percentile by over 1°C are picked
 554 out afterwards over the Amery ice shelf on 22/23 March 2022, perhaps associated with the atmospheric river
 555 moving from west to east around East Antarctica but reducing in intensity as it headed between Totten and Amery.
 556 As this atmospheric river primarily affected East Antarctica, it does not show up as an extreme weather event
 557 over the other ice shelves.



558

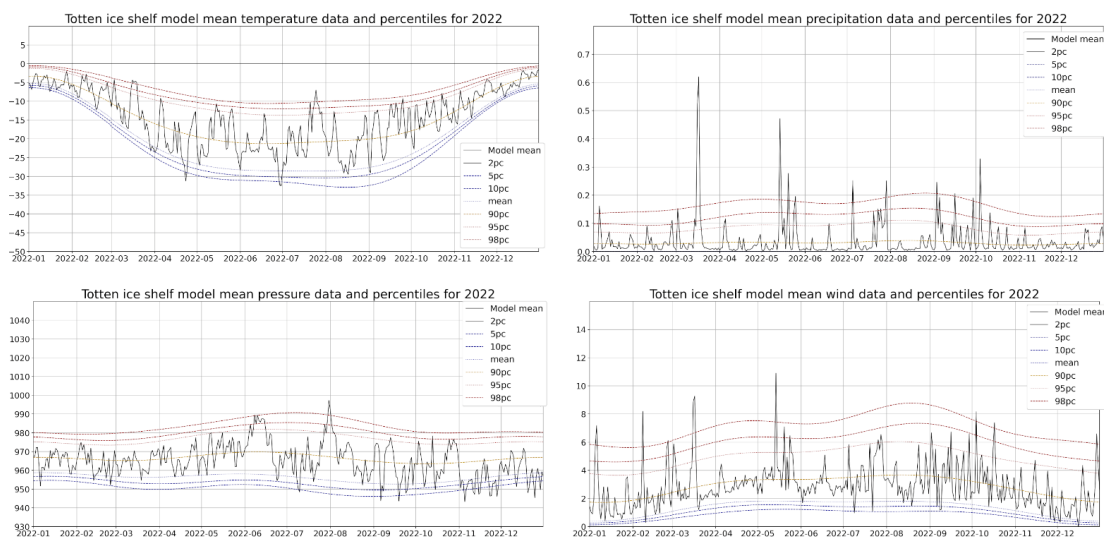


Figure 11. RACMO2 simulated daily surface temperature (°C), precipitation (mm), surface pressure (hPa) and wind speed (m/s) data for 2022, and daily percentiles from 2001 to 2019, for the Totten Ice Shelf.

559

560

5. Discussion

561 We have developed a database of Antarctic meteorological extremes that identifies a succession of warm
 562 summers in the mid to late 1990s, especially over the Antarctic Peninsula and West Antarctica, followed by a lull
 563 in the late 2000s and early 2010s, and then an increase again after around 2015. This is reflected both in the mean
 564 temperature time series and in the distributions of extreme temperature events, with most of the ice shelves
 565 considered having at least one extreme year for high temperature events between 1995 and 1998, and having at
 566 least one more in 2016, 2019 and/or 2020. Although several of the ice shelves had exceptional warm years in
 567 1998 and 2016, which corresponded to strong El Nino events, there does not appear to be a strong overall link
 568 between high temperatures and ENSO in most cases.

569 While many of the known extreme ice shelf melt or breakup events over the ice shelves correspond to extreme
 570 values of temperature, precipitation, wind or pressure, some do not, such as the disintegration of Larsen B in
 571 early 2002 (van den Broeke, 2005), and the calving event over the Amery ice shelf on 25 September 2019 (Francis
 572 et al., 2022). It is possible that the extreme conditions in the Weddell Sea documented by Turner et al. (2017)
 573 may not have strongly affected the Amery ice shelf directly and that impacts from the ocean may have been a
 574 more important cause than the surface weather over Amery. However, for example, the disintegration of Larsen
 575 A in January 1995, the extreme melt over George VI in summer 2019/20, and the atmospheric river of March
 576 2022, do correspond to extreme weather events in the database. The mean sea level pressure anomaly for January
 577 1995 (Figure 7) shows below-average pressure over much of Antarctica but a high pressure anomaly off the coast



578 of the Peninsula which implies that westerly winds blew more strongly and/or frequently than usual over the
579 Peninsula. These conditions are also potentially conducive to a föhn effect over the Larsen ice shelf, and föhn
580 winds over Larsen can be linked with extreme melt episodes (Turton et al. 2020). The database also shows up
581 the succession of warm summers that preceded and probably contributed to the disintegration of Larsen B (for
582 example van den Broeke, 2005).

583 There were other months with repeated extreme meteorological events that did not have widely documented
584 impacts on the Antarctic ice shelves, such as February 2006, which was associated with intense melting on Peter
585 1st Island, and March 2017. Presumably in these cases, temperatures were not generally high enough for long
586 enough to have a substantial impact on the affected ice shelves. However, events such as these are worth
587 monitoring because in a warmer future climate, these events may bring rain instead of snow to parts of the affected
588 ice shelves, leading to them being associated with substantial melting and calving events in the future (Wille et
589 al. 2024b, Chan et al. 2023).

590 Over the period considered (1995-2023), the results suggested that low sea ice extent over neighbouring seas
591 tended not to be significantly linked with an increased number of extreme temperature or precipitation events,
592 which also implies that caution is needed over linking recent extreme events to reduced sea ice cover. However,
593 the links could become statistically significant if a longer period is used. There is also potential for this to change
594 in a future warmer climate, should Antarctic sea ice become persistently low, combined with the general warming
595 trend in the global climate (Wille et al. 2024a).

596 There was little evidence for an increase in extreme weather events over the period, but signs that, especially for
597 the Peninsula and West Antarctica, we may have seen a decline in extreme events as well as mean temperatures
598 between around 1995 and 2010, followed by another increase since around 2015, which may be linked with
599 variations in the Interdecadal Pacific Oscillation and allied variability in the Amundsen sea low (Meehl et al.
600 2016). As with the exceptionally low surrounding sea ice extent of recent years, it is currently too early to
601 determine whether this increase since 2015 is associated mainly with short term variability or whether it is the
602 beginning of a long-term climatic shift.

603

604 6. Conclusions

605 Using daily, monthly, seasonal and annual temperature, precipitation, wind and pressure from existing
606 simulations with four RCMs, we have created a novel database of Antarctic extreme weather events over eight
607 key Antarctic ice shelves. These extreme events often, but not always, align with notable melting and calving
608 events over the ice shelves. There is no clear evidence of an increase in extreme weather events over the period
609 1995-2023, but in many cases there is evidence of a decline in extreme events between around 1995 and 2010,
610 followed by an increase since then, albeit not to higher levels than these ice shelves saw in the mid to late 1990s.

611 It would be useful to extend the analysis back into the 1980s to determine whether the well-documented upward
612 trend in mean temperatures in the Antarctic Peninsula is matched by a long-term increase in extreme weather



613 events. As only one model was available for the 1980s and early 1990s (RACMO2), we chose not to look at
614 RACMO2 before 1995 for this paper, but the full set of RACMO2 data will be the subject of future work. The
615 extremes database produced here is expected to be of use for validating model simulations of extremes against
616 observations, which may provide useful insights for future development of model simulations over Antarctica
617 and the surrounding region. The database also provides information which can be used to assist case-study
618 analysis, such as of conditions leading up to and during ice-shelf breakup events or exceptional heatwaves or
619 melt events. The extremes database can also be used to help assess the weather system drivers of extreme events,
620 looking at temperature, precipitation, surface wind speeds and surface pressure. For example, atmospheric river
621 catalogues, storm track and blocking databases and empirical orthogonal function analysis can be used to make
622 comparisons with extreme events that are picked out in the database.

623

624

Author contributions

625 Ian Simpson wrote the manuscript draft and produced and analysed the extremes database. Edward Hanna, Ruam
626 Williams, Linh Luu, Andrew Orr, Julie Jones and Xavier Fettweis reviewed and edited the manuscript. Julie
627 Jones, Edward Hanna, Sihan Li and Andrew Orr raised funding for the project. Jose Abraham Torres Alavez, Ole
628 Bøssing Christensen, Xavier Fettweis, Ella Gilbert, Sid Gumber, Christoph Kittel, Damien Maure, Ruth Mottram,
629 Tony Phillips, Willem Jan van de Berg and Kristiina Verro provided the regional climate model simulations.

630

631

Competing interests

632 At least one of the co-authors is a member of the editorial board of *The Cryosphere*. There are no other competing
633 interests to declare.

634

635

Acknowledgements

636 Many thanks to Thomas Bracegirdle for providing code for the 3-point harmonic filter used for the daily
637 percentiles, and to Sergey Chulkov for considerable technical support to the work behind this paper. We
638 acknowledge NERC grant PICANTE, NE/Y503290/1.

639 We also thank the Koninklijk Nederlands Meteorologisch Instituut (KNMI) for providing RACMO2 model
640 simulations, the Danmarks Meteorologiske Institut (DMI) for providing HCLIM model simulations, the British
641 Antarctic Survey (BAS) for the MetUM model simulations, and the University of Liège for the MAR model
642 simulations. We also thank the team at BAS for the extensive work on the PolarRES ensemble and for making
643 Antarctic station data available via READER, and ECMWF for providing the ERA5 reanalysis which forms the
644 basis for some of the plots.

645



646

Data availability statement

647 It is anticipated that the database of Antarctic meteorological extremes will be made available at the Centre for
648 Environmental Data Analysis (CEDA) following the end of the research grant for the analysis in 2028. Prior to
649 this time, the database will be available upon request from the primary corresponding author.

650

651

References

- 652 Baiman, R., Winters, A. C., Mayer, K. J., & Reiher, C. A. (2025). Disentangling regional drivers of top
653 Antarctic snowfall days with a convolutional neural network. *Geophysical Research Letters*, 52,
654 e2025GL115254. <https://doi.org/10.1029/2025GL115254>
- 655 Banwell, A. F., Datta, R. T., Dell, R. L., Moussavi, M., Brucker, L., Picard, G., Shuman, C. A., and Stevens, L.
656 A.: The 32-year record-high surface melt in 2019/2020 on the northern George VI Ice Shelf, Antarctic
657 Peninsula, *The Cryosphere*, 15, 909–925, <https://doi.org/10.5194/tc-15-909-2021>, 2021.
- 658 Belušić, D., de Vries, H., Dobler, A., Landgren, O., Lind, P., Lindstedt, D., Pedersen, R. A., Sánchez-Perrino, J.
659 C., Toivonen, E., van Ulft, B., Wang, F., Andrae, U., Batrak, Y., Kjellström, E., Lenderink, G., Nikulin, G.,
660 Pietikäinen, J.-P., Rodríguez-Camino, E., Samuelsson, P., van Meijgaard, E., and Wu, M.: HCLIM38: a
661 flexible regional climate model applicable for different climate zones from coarse to convection-permitting
662 scales, *Geosci. Model Dev.*, 13, 1311–1333, <https://doi.org/10.5194/gmd-13-1311-2020>, 2020.
- 663 Bracegirdle, T.J., Caton Harrison, T., Holmes, C.R. et al. Antarctic extreme seasons under 20th and 21st
664 century climate change. *npj Clim Atmos Sci* 7, 276 (2024). <https://doi.org/10.1038/s41612-024-00822-y>
- 665 Carrasco, J. F., Bozkurt, D., & Cordero, R. R. (2021). A review of the observed air temperature in the Antarctic
666 Peninsula. Did the warming trend come back after the early 21st hiatus? *Polar Science*, 28, 100653.
- 667 Chan, A. C., England, M. R., Screen, J. A., Bracegirdle, T. J., Blockley, E. W., & Holmes, C. R. (2025).
668 Extreme Antarctic sea ice loss facilitated by negative shift of Southern Annular Mode. *Geophysical Research*
669 *Letters*, 52, e2025GL116688. <https://doi.org/10.1029/2025GL116688>
- 670 Clem, K.R., Bozkurt, D., Kennett, D. et al. Central tropical Pacific convection drives extreme high
671 temperatures and surface melt on the Larsen C Ice Shelf, Antarctic Peninsula. *Nat Commun* 13, 3906 (2022).
672 <https://doi.org/10.1038/s41467-022-31119-4>
- 673 Clem, K. R., et al. (2023). Antarctica and the Southern Ocean. *Bull. Amer. Meteor. Soc.*, 104, S322–
674 S365, <https://doi.org/10.1175/BAMS-D-23-0077.1>.
- 675 Christiaan T. van Dalum, Willem Jan van de Berg, Srinidhi N. Gadde, Maurice van Tiggelen, Tijmen van der
676 Drift, Erik van Meijgaard, Lambertus H. van Ulft, and Michiel R. van den Broeke, *The Cryosphere*, 18, 4065–
677 4088, <https://doi.org/10.5194/tc-18-4065-2024>
- 678 Dethinne, T., Glaude, Q., Picard, G., Kittel, C., Alexander, P., Orban, A. and Fettweis, X. (2023). Sensitivity of



- 679 the MAR regional climate model snowpack to the parameterization of the assimilation of satellite-derived wet-
680 snow masks on the Antarctic Peninsula. *The Cryosphere*. 17. 4267-4288. 10.5194/tc-17-4267-2023.
- 681 Fahnestock, M. A., Abdalati, W. & Shuman, C. A. Long melt seasons on ice shelves of the Antarctic Peninsula:
682 an analysis using satellite-based microwave emission measurements. *Ann. Glaciol.* **34**, 127–133 (2002).
- 683 Francis, D., Mattingly, K. S., Lhermitte, S., Temimi, M., and Heil, P.: Atmospheric extremes caused high
684 oceanward sea surface slope triggering the biggest calving event in more than 50 years at the Amery Ice Shelf,
685 *The Cryosphere*, 15, 2147–2165, <https://doi.org/10.5194/tc-15-2147-2021>, 2021.
- 686 Francis, D., Fonseca, R., Mattingly, K. S., Marsh, O. J., Lhermitte, S., & Cherif, C. (2022). Atmospheric
687 triggers of the Brunt Ice Shelf calving in February 2021. *Journal of Geophysical Research: Atmospheres*, 127,
688 e2021JD036424. <https://doi.org/10.1029/2021JD036424>
- 689 Gerrish, L., Fretwell, P., and Cooper, P. (2020). High resolution vector polygons of the Antarctic coastline -
690 VERSION 7.2 (Version 7.2) [Data set]. UK Polar Data Centre, Natural Environment Research Council, UK
691 Research & Innovation. <https://doi.org/10.5285/065b9abc-1b5a-4fc6-aa57-9052428aa6ca>
- 692 Gilbert, E., Abraham Torres-Alavez, J., Hofsteenge, M.G., et al. The PolarRES dataset: a state-of-the-art
693 regional climate model ensemble for understanding Antarctic climate. (Preprint). To be published in *The*
694 *Cryosphere*. Available from [https://egusphere.copernicus.org/preprints/2025/egusphere-2025-4214/egusphere-](https://egusphere.copernicus.org/preprints/2025/egusphere-2025-4214/egusphere-2025-4214.pdf)
695 [2025-4214.pdf](https://egusphere.copernicus.org/preprints/2025/egusphere-2025-4214/egusphere-2025-4214.pdf). Accessed 04 November 2025.
- 696 Glasser NF, Scambos TA. A structural glaciological analysis of the 2002 Larsen B ice-shelf collapse. *Journal*
697 *of Glaciology*. 2008;54(184):3-16. doi:10.3189/002214308784409017
- 698 González-Herrero, S., Barriopedro, D., Trigo, R.M. *et al.* Climate warming amplified the 2020 record-breaking
699 heatwave in the Antarctic Peninsula. *Commun Earth Environ* **3**, 122 (2022). [https://doi.org/10.1038/s43247-](https://doi.org/10.1038/s43247-022-00450-5)
700 [022-00450-5](https://doi.org/10.1038/s43247-022-00450-5)
- 701 Gorodetskaya, I.V., Durán-Alarcón, C., González-Herrero, S. *et al.* Record-high Antarctic Peninsula
702 temperatures and surface melt in February 2022: a compound event with an intense atmospheric river. *npj Clim*
703 *Atmos Sci* **6**, 202 (2023). <https://doi.org/10.1038/s41612-023-00529-6>
- 704 Hall, R. J., J. M. Jones, R. L. Fogt, and T. J. Bracegirdle, 2025: Variability and Trends of the Amundsen Sea
705 Low since the Early Twentieth Century from Seasonal-Station-Based Reconstructions. *J. Climate*, **38**, 7509–
706 7527, <https://doi.org/10.1175/JCLI-D-25-0159.1>.
- 707 Hanna, E., et al. (2011), Greenland Ice Sheet surface mass balance 1870 to 2010 based on Twentieth Century
708 Reanalysis, and links with global climate forcing, *J. Geophys. Res.*, 116, D24121, doi:10.1029/2011JD016387
- 709 Hanna, E., Topál, D., Box, J.E. *et al.* Short- and long-term variability of the Antarctic and Greenland ice
710 sheets. *Nat Rev Earth Environ* **5**, 193–210 (2024). <https://doi.org/10.1038/s43017-023-00509-7>
- 711 Hersbach H, Bell B, Berrisford P, et al. The ERA5 global reanalysis. *Q J R Meteorol Soc.* 2020; 146: 1999–
712 2049. <https://doi.org/10.1002/qj.3803>



- 713 Josey, S.A., Meijers, A.J.S., Blaker, A.T. *et al.* Record-low Antarctic sea ice in 2023 increased ocean heat loss
714 and storms. *Nature* **636**, 635–639 (2024). <https://doi.org/10.1038/s41586-024-08368-y>
- 715 King, J., Anchukaitis, K.J., Allen, K. *et al.* Trends and variability in the Southern Annular Mode over the
716 Common Era. *Nat Commun* **14**, 2324 (2023). <https://doi.org/10.1038/s41467-023-37643-1>
- 717 Kolbe, M., Torres Alavez, J.A., Mottram, R. *et al.* Atmospheric rivers and winter sea ice drive recent reversal
718 in Antarctic ice mass loss. *Commun Earth Environ* **7**, 255 (2026). <https://doi.org/10.1038/s43247-026-03242-3>
- 719 Lai, C.Y., Kingslake, J., Wearing, M.G. *et al.* Vulnerability of Antarctica’s ice shelves to meltwater-driven
720 fracture. *Nature* **584**, 574–578 (2020). <https://doi.org/10.1038/s41586-020-2627-8>
- 721 Li, X., Cai, W., Meehl, G.A. *et al.* Tropical teleconnection impacts on Antarctic climate changes. *Nat Rev*
722 *Earth Environ* **2**, 680–698 (2021). <https://doi.org/10.1038/s43017-021-00204-5>
- 723 Marshall, G. J., 2003: Trends in the Southern Annular Mode from observations and reanalyses. *J.*
724 *Clim.*, **16**, 4134–4143, doi:10.1175/1520-0442%282003%29016<4134%3ATITSAM>2.0.CO%3B2
- 725 Massom, R.A., Scambos, T.A., Bennetts, L.G. *et al.* Antarctic ice shelf disintegration triggered by sea ice loss
726 and ocean swell. *Nature* **558**, 383–389 (2018). <https://doi.org/10.1038/s41586-018-0212-1>
- 727 Meier, Walter N., and J. Scott Stewart. (2023). NSIDC Land, Ocean, Coast, Ice, and Sea Ice Region Masks.
728 NSIDC Special Report 25. Boulder CO, USA: National Snow and Ice Data Center.
729 <https://nsidc.org/sites/default/files/documents/technical-reference/nsidc-special-report-25.pdf>.
- 730 Meehl, G. A., Arblaster, J. M., Bitz, C. M., Chung, C. T. Y. & Teng, H. Antarctic sea-ice expansion between
731 2000 and 2014 driven by tropical Pacific decadal climate variability. *Nature Geosci* **9**, 590–595 (2016).
- 732 Mottram, R., Hansen, N., Kittel, C., van Wessem, J. M., Agosta, C., Amory, C., Boberg, F., van de Berg, W. J.,
733 Fettweis, X., Gossart, A., van Lipzig, N. P. M., van Meijgaard, E., Orr, A., Phillips, T., Webster, S., Simonsen,
734 S. B., and Souverijns, N.: What is the surface mass balance of Antarctica? An intercomparison of regional
735 climate model estimates, *The Cryosphere*, **15**, 3751–3784, <https://doi.org/10.5194/tc-15-3751-2021>, 2021.
- 736 Narapusetty, B., T. DelSole, and M. K. Tippett, 2009: Optimal Estimation of the Climatological Mean. *J.*
737 *Climate*, **22**, 4845–4859, <https://doi.org/10.1175/2009JCLI2944.1>.
- 738 Nicolas, J., Vogelmann, A., Scott, R. *et al.* January 2016 extensive summer melt in West Antarctica favoured
739 by strong El Niño. *Nat Commun* **8**, 15799 (2017). <https://doi.org/10.1038/ncomms15799>
- 740 Orr, A., *et al.* (2023): Characteristics of Surface “Melt Potential” over Antarctic Ice Shelves based on Regional
741 Atmospheric Model Simulations of Summer Air Temperature Extremes from 1979/80 to 2018/19. *J.*
742 *Climate*, **36**, 3357–3383, <https://doi.org/10.1175/JCLI-D-22-0386.1>.
- 743 Ootosaka, I. N., Shepherd, A., Ivins, E. R., Schlegel, N.-J., *et al.* Mass balance of the Greenland and Antarctic
744 ice sheets from 1992 to 2020, *Earth Syst. Sci. Data*, **15**, 1597–1616, <https://doi.org/10.5194/essd-15-1597-2023>,
745 2023.
- 746 Pezza, A.B., Rashid, H.A. & Simmonds, I. Climate links and recent extremes in antarctic sea ice, high-latitude



- 747 cyclones, Southern Annular Mode and ENSO. *Clim Dyn* **38**, 57–73 (2012). <https://doi.org/10.1007/s00382-011->
748 1044-y
- 749 Rignot, E., Larour, E., Scheuchl, B., Poinelli, M. (2021). Physical processes controlling the rifting of Larsen C
750 Ice Shelf, Antarctica, prior to the calving of iceberg A68 in 2017 [Dataset].
751 Dryad. <https://doi.org/10.7280/D1TX1F>
- 752 Risien, C. M., and D. B. Chelton, 2008: A Global Climatology of Surface Wind and Wind Stress Fields from
753 Eight Years of QuikSCAT Scatterometer Data. *J. Phys. Oceanogr.*, **38**, 2379–
754 2413, <https://doi.org/10.1175/2008JPO3881.1>.
- 755 Rogers, J. C., and H. van Loon, 1982: Spatial Variability of Sea Level Pressure and 500 mb Height Anomalies
756 over the Southern Hemisphere. *Mon. Wea. Rev.*, **110**, 1375–1392, <https://doi.org/10.1175/1520->
757 [0493\(1982\)110<1375:SVOSLP>2.0.CO;2](https://doi.org/10.1175/1520-0493(1982)110<1375:SVOSLP>2.0.CO;2).
- 758 Royston, S., Gudmundsson, G.H. (2016) Changes in ice-shelf buttressing following the collapse of Larsen A
759 Ice Shelf, Antarctica, and the resulting impact on tributaries. *Journal of Glaciology*. 2016;62(235):905-911.
760 doi:10.1017/jog.2016.77
- 761 Scambos, T. A., J. A. Bohlander, C. A. Shuman, and P. Skvarca (2004), Glacier acceleration and thinning after
762 ice shelf collapse in the Larsen B embayment, Antarctica, *Geophys. Res. Lett.*, **31**, L18402,
763 doi:[10.1029/2004GL020670](https://doi.org/10.1029/2004GL020670).
- 764 Scambos, T., H.A. Fricker, C.-C. Liu, J. Bohlander, J. Fastook, A. Sargent, R. Massom, and A.-M. Wu. 2009.
765 Ice shelf disintegration by plate bending and hydro-fracture: Satellite observations and model results of the
766 2008 Wilkins ice shelf break-ups. *Earth and Planetary Science Letters*, **280**: 51-
767 60. <https://doi.org/10.1016/j.epsl.2008.12.027>
- 768 Scambos TA, Hulbe C, Fahnestock M, Bohlander J. The link between climate warming and break-up of ice
769 shelves in the Antarctic Peninsula. *Journal of Glaciology*. 2000;46(154):516-530.
770 doi:10.3189/172756500781833043
- 771 Siegert MJ, Bentley MJ, Atkinson A, Bracegirdle TJ, Convey P, Davies B, Downie R, Hogg AE, Holmes C,
772 Hughes KA, Meredith MP, Ross N, Rumble J and Wilkinson J (2023), Antarctic extreme events. *Front.*
773 *Environ. Sci.* **11**:1229283. doi: 10.3389/fenvs.2023.1229283
- 774 Thomas, E. R., Tetzner, D., Markle, B., Pedro, J., Gacit'ua, G., Moser, D. E., Jackson, S. (2024). The first firn
775 core from Peter I Island -- capturing climate variability across the Bellingshausen Sea. *Climate of the Past* (20)
776 (11), pp. 2525-2538, doi: 10.5194/cp-20-2525-2024
- 777 Thompson, D. W. J., and J. M. Wallace, 2000: Annular Modes in the Extratropical Circulation. Part I: Month-
778 to-Month Variability. *J. Climate*, **13**, 1000–1016, <https://doi.org/10.1175/1520->
779 [0442\(2000\)013<1000:AMITEC>2.0.CO;2](https://doi.org/10.1175/1520-0442(2000)013<1000:AMITEC>2.0.CO;2).
- 780 Turner, J., et al. (2004). The SCAR READER Project: Toward a High-Quality Database of Mean Antarctic
781 Meteorological Observations. *J. Climate*, **17**, 2890–2898, <https://doi.org/10.1175/1520->



- 782 [0442\(2004\)017<2890:TSRPTA>2.0.CO;2](https://doi.org/10.1029/2009GL037524).
- 783 Turner, J., J. C. Comiso, G. J. Marshall, T. A. Lachlan-Cope, T. Bracegirdle, T. Maksym, M. P. Meredith, Z.
784 Wang, and A. Orr (2009), Non-annular atmospheric circulation change induced by stratospheric ozone
785 depletion and its role in the recent increase of Antarctic sea ice extent, *Geophys. Res. Lett.*, 36, L08502,
786 doi:[10.1029/2009GL037524](https://doi.org/10.1029/2009GL037524).
- 787 Turner, J., Lu, H., White, I. *et al.* Absence of 21st century warming on Antarctic Peninsula consistent with
788 natural variability. *Nature* **535**, 411–415 (2016). <https://doi.org/10.1038/nature18645>
- 789 Turner, J., Comiso, J. Solve Antarctica’s sea-ice puzzle. *Nature* **547**, 275–277 (2017).
790 <https://doi.org/10.1038/547275a>
- 791 Turner, J., Guarino, M. V., Arnatt, J., Jena, B., Marshall, G. J., Phillips, T., et al. (2020). Recent decrease of
792 summer sea ice in the Weddell Sea, Antarctica. *Geophysical Research Letters*, 47, e2020GL087127.
793 <https://doi.org/10.1029/2020GL087127>
- 794 Turton, J. V., Kirchgassner, A., Ross, A. N., King, J. C., and Kuipers Munneke, P.: The influence of föhn
795 winds on annual and seasonal surface melt on the Larsen C Ice Shelf, Antarctica, *The Cryosphere*, 14, 4165–
796 4180, <https://doi.org/10.5194/tc-14-4165-2020>, 2020.
- 797 van den Broeke, M. (2005), Strong surface melting preceded collapse of Antarctic Peninsula ice shelf,
798 *Geophys. Res. Lett.*, 32, L12815, doi:[10.1029/2005GL023247](https://doi.org/10.1029/2005GL023247).
- 799 van Wessem, J.M., van den Broeke, M.R., Wouters, B. *et al.* Variable temperature thresholds of melt pond
800 formation on Antarctic ice shelves. *Nat. Clim. Chang.* **13**, 161–166 (2023). [https://doi.org/10.1038/s41558-022-](https://doi.org/10.1038/s41558-022-01577-1)
801 [01577-1](https://doi.org/10.1038/s41558-022-01577-1)
- 802 Wang, Y. et al., (2025), Deep learning, the flow law of Antarctic ice shelves. *Science* 387, 1219-
803 1224(2025). DOI:10.1126/science.adp3300
- 804 Wang, Z., J. Turner, Y. Wu, and C. Liu, 2019: Rapid Decline of Total Antarctic Sea Ice Extent during 2014–16
805 Controlled by Wind-Driven Sea Ice Drift. *J. Climate*, **32**, 5381–5395, [https://doi.org/10.1175/JCLI-D-18-](https://doi.org/10.1175/JCLI-D-18-0635.1)
806 [0635.1](https://doi.org/10.1175/JCLI-D-18-0635.1).
- 807 Wille, J. D., and Coauthors, 2024a: The Extraordinary March 2022 East Antarctica “Heat” Wave. Part I:
808 Observations and Meteorological Drivers. *J. Climate*, **37**, 757–778, <https://doi.org/10.1175/JCLI-D-23-0175.1>.
- 809 Wille, J. D., and Coauthors, 2024b: The Extraordinary March 2022 East Antarctica “Heat” Wave. Part II:
810 Impacts on the Antarctic Ice Sheet. *J. Climate*, **37**, 779–799, <https://doi.org/10.1175/JCLI-D-23-0176.1>.
- 811 Xu, M., Yu, L., Liang, K. *et al.* Dominant role of vertical air flows in the unprecedented warming on the
812 Antarctic Peninsula in February 2020. *Commun Earth Environ* **2**, 133 (2021). [https://doi.org/10.1038/s43247-](https://doi.org/10.1038/s43247-021-00203-w)
813 [021-00203-w](https://doi.org/10.1038/s43247-021-00203-w)
- 814 Zhang, T, A. Hoell, J. Perlwitz, J. Eischeid, D. Murray, M. Hoerling and T. Hamill, 2019: Towards
815 Probabilistic Multivariate ENSO Monitoring, *Geophys. Res. Lett.*, 46, DOI: 10.1029/2019GL083946

<https://doi.org/10.5194/egusphere-2026-2270>

Preprint. Discussion started: 1 June 2026

© Author(s) 2026. CC BY 4.0 License.



816 Zhu, Z., & Song, M. (2023). Impacts of Observed Extreme Antarctic Sea Ice Conditions on the Southern
817 Hemisphere Atmosphere. *Atmosphere*, 14(1), 36. <https://doi.org/10.3390/atmos14010036>
818